JST: Engineering and Technology for Sustainable Development
Volume 34, Issue 4, October 2024, 009-016

Production of Porous Silica from Rice Husk Using Cetyltrimethylammonium Bromide to Remove Dyes in Aqueous Solution

Nguyen Van Doan[1], Nguyen Thi Mai[1], Dao Thi Cam Vi[1], Nguyen Thu Huong[1], Vu Tuan Cuong[2], Le Trung Phong[2], Nguyen Thu Huyen[2], Vu Anh Tuan[1*]

[1]School of Chemistry and Life Sciences, Hanoi University of Science and Technology, Ha Noi, Vietnam
[2]Nguyen Gia Thieu High School, Ha Noi, Vietnam
[*]Corresponding author email: tuan.vuanh@hust.edu.vn

Abstract

Porous silica was prepared from rice husk (RH) for the removal of organic dye (Janus Green B, JGB). The as-prepared samples were analyzed by using emission scanning electron microscope (SEM), transmission electron microscopy (TEM), X-ray diffraction (XRD), and N_2 adsorption/desorption isotherm. The as-prepared silica was an amorphous and mesoporous material and the textural properties depended on the assistance of cetyltrimethylammonium bromide (CTAB). The SiO_2-15 sample had a large surface area of 544.5 m^2/g, a high pore volume of 1.259 cm^3/g and average pore size of 9.4 nm. The performance of the SiO_2-15 was evaluated by the removal of JGB and the effects of reaction parameters on the adsorption process were extensively explored. The optimum conditions for the removal of JGB were adsorbent dosage of 0.5 g/L, solution pH of 6, JGB concentration of 30 ppm, and temperature of 30 °C. The removal efficiency of JGB on SiO_2-15 was 98.83% in 60 min with a rate constant of 0.025 $g.mg^{-1}.min^{-1}$. In addition, the adsorption is fast in the initial 5 min and the adsorption isotherms were investigated.

Keywords: Adsorption, porous silica, rice husks, CTAB, Janus Green B.

1. Introduction

Pollution from organic compounds is a major problem worldwide. The cause of this situation could be the significant increase in the use of synthetic dyes in industry in recent years. According to the World Health Organization (WHO), around 1.1 billion people worldwide still do not have access to clean water and around 2.4 billion people lack access to adequate sanitation [1]. In many cases, industrial wastewater is not only discharging directly, but also infiltrating into the ground, polluting underground water sources. Therefore, the removal of dyes from contaminated water become important and necessary to eliminate potential hazards. Jannus Green B (JGB) belongs to the group of azo dyes, which is one of the most typical dyes widely used in various industries [2]. They prevent photosynthesis and affect aquatic systems by limiting the transmission of sunlight into water. JGB is often chosen in studies to evaluate the adsorption efficiency of materials.

The adsorption method has been extensively studied as an optimal measure for wastewater treatment due to its simplicity, easy operation, and high efficiency [3]. Silica is an excellent choice for wastewater treatment due to its high stability, large surface area and low cost [4]. Many porous silica composites have been synthesized for the removal of organic compounds such as acid red, dimethyl phthalate, methyl blue, and acid dyes [5, 6]. Porous silica can be synthesized from raw material sources such as tetraethyl orthosilicate (TEOS) [7]. However, some of the disadvantages of this raw material is that it is quite expensive and dangerous because it is flammable. Recently, rice husk (RH), an agricultural waste product and a cheap source of silica, have been produced in enormous quantities as a by-product of rice mills. Rice husk ash (RHA) in particular contains around 90 wt.% of silica, which is an economically valuable raw material for the production of natural silica.

Some porous materials are created from the formation of surfactant micelles. The surfactant commonly used in the formation of mesoporous materials was cetyltrimethylammonium bromide (CTAB), a cationic surfactant. They act as pore molds that support the production of surfaces with porous structure after being processed at high temperature. In this study, porous silica was prepared from rice husk (RH) by hydrothermal method using CTAB. The as-prepared samples were characterized by scanning electron microscope (SEM), transmission electron microscopy (TEM), X-ray diffraction (XRD), and

ISSN 2734-9381
https://doi.org/10.51316/jst.177.etsd.2024.34.4.2
Received: Mar 18, 2024; revisesd: Jun 14, 2024;
accepted: Jul 25, 2024.

nitrogen adsorption/desorption isotherms. The adsorption of SiO_2 was evaluated by the adsorption of JGB.

2. Experiment

2.1. Materials

Janus Green B (JGB, 99%) was purchased from Sigma-Aldrich, the chemical structure and basic physicochemical properties of JGB are presented in Fig. 1(a). Rice husk was obtained from Lo Giang, Dong Hung, Thai Binh, Viet Nam. Sodium hydroxide (99.5%), cetyltrimethylammonium bromide (CTAB, 99%) were obtained from India, the chemical structure of CTAB is presented in Fig. 1(b). The pH of the solution was adjusted by using dilute solutions of H_2SO_4 and NaOH.

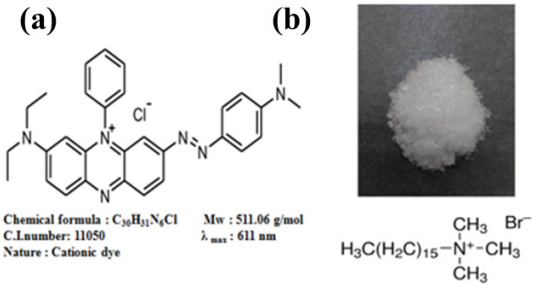

Fig. 1. (a) The chemical structure and physical properties of JGB, (b) CTAB

2.2. Synthesis of Silica

The synthesis process is depicted in Fig. 2 (a, b) [8]. The RH was washed with tap water and then rinsed 6 to 7 times with distilled water. The washed RH was soaked separately with 0.5 M HCl for 30 min and shaken continuously. After the acidic solution was completely removed, the RH was rinsed with distilled water, filtered and dried at 100 °C for 24 h. It was then combusted in a muffle furnace at 600 °C for 2 h to obtain RHA. After that, 5 g of RHA was weighed into an Erlenmeyer flask containing 100 mL of 2 N NaOH. The mixture was stirred at 60 °C for 2 h and then filtered to obtain the Na_2SiO_3 solution in Fig. 2(a).

To investigate the influence of CTAB content on the adsorption of JGB, the SiO_2 samples were synthesized with different doses of CTAB. Typically, 34 mL of 0.6 M HCl and CTAB (0.21867, 1.0934, 2.1867 and 3.2801 g) were mixed in a 250 mL beaker and stirred until all substances were completely dissolved, 40 mL of Na_2SiO_3 solution was added to the beaker and adjusted to pH=7.5-8.5 by HCl. The mixture was incubated for 24 h at 50 °C to obtain a white gel and then hydrothermally heated at 100 °C for 48 h. The white powder was obtained by filtering and washing and dried overnight at 100 °C and then calcined at 600 °C for 6 h (Fig. 2 (b)). The as-synthesized samples designated as SiO_2-1, SiO_2-5, SiO_2-10 and SiO_2-15 for CTAB doses of 0.2187, 1.0934, 2.1867 and 3.2801 g, respectively. For comparising, the sample without CTAB was prepared and designated as SiO_2-0.

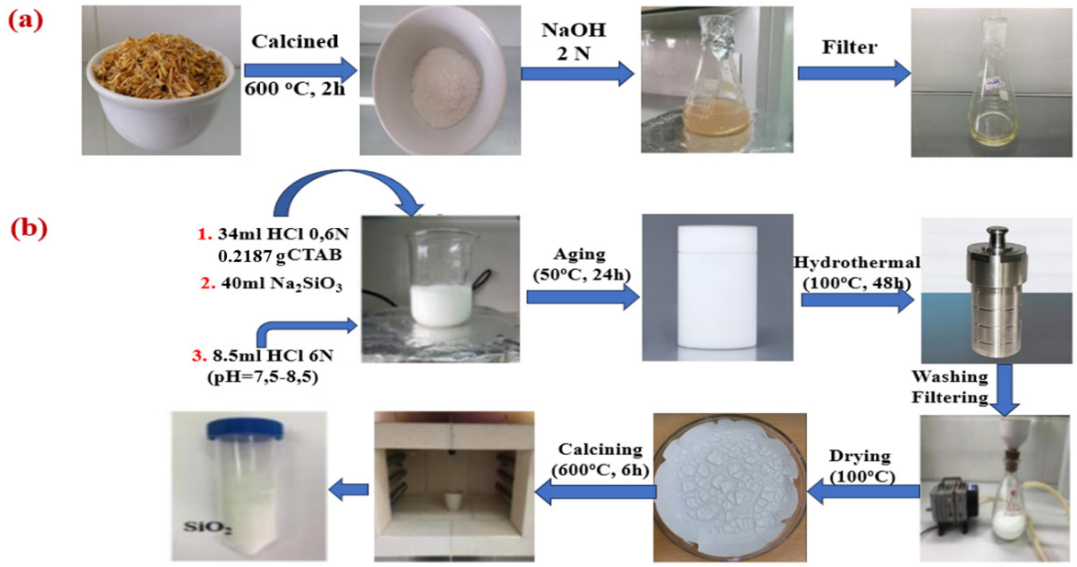

Fig. 2. Schemes for the synthesis of (a) Na_2SiO_3, (b) SiO_2

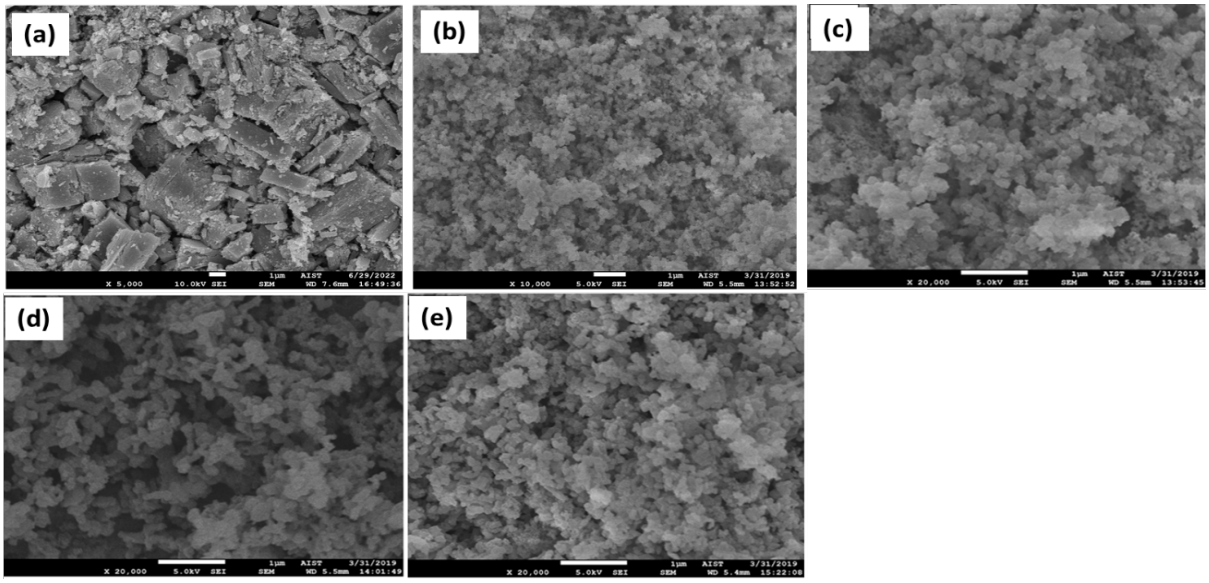

Fig. 3. SEM images of (a) SiO_2-0, (b) SiO_2-1, (c) SiO_2-5, (d) SiO_2-10, (e) SiO_2-15.

2.3. Characterizations

The X-ray diffraction (XRD) analysis were used to determine the crystalline phase of the material. Measurements using a Bruker D8 Advance diffractometer (Germany) with Cu-Kα irradiation (40 kV and 40 mA) at 2θ between 5 and 80°. The morphology and size of the samples were investigated by transmission electron microscopy (TEM, JEM-JEOL 2100) and emission scanning electron microscopy (SEM, JEOL-7600F). The specific surface area of the sample was measured using the nitrogen adsorption/desorption isotherm method.

2.4. Adsorption Experiment

The dye concentration of the filtrate was analyzed by a UV-Vis spectrophotometer (Agilent 8453) at the maximum absorbance wavelength 611 nm. A beaked glass beaker was used to hold 100 mL of JGB solution at a specific concentration and an amount of SiO_2. The suspension was placed on a magnetic stirrer at 250 rpm. At given time intervals, 2 mL of samples were withdrawn from the suspension and then filtered by a syringe filter (0.45 µm PTFE membrane) to remove the adsorbent. The removal efficiency (R_e) and adsorption capacity (q_e) of the sample was determined using the following equation [9]:

$$R_e = \frac{C_0 - C_t}{C_0} \times 100\% \quad (1)$$

$$q_{e,cal} = \frac{(C_0 - C_e).V}{m} \quad (2)$$

where C_o (mg/L) is the initial dye concentration, C_e (mg/L) is the dye concentration at equilibrium and C_t (mg/L) is the concentration at adsorption time t, V is the volume of dye solution (L), m is the mass of the adsorbent (g).

3. Results and Discussion

3.1. Influence of CTAB Content on Characterization of Silica

3.1.1. SEM analysis

The morphology and composition of the samples are expressed in Fig. 3(a-d). Calcination at 600 ºC results in a well-defined boundary for the silica sample without addition of CTAB (SiO_2-0) and it has the solid bulk shape. For the samples with addition of CTAB, it can be easily observed that the silica particles have a spherical shape and uniform size. Many silica nanoparticles clump together to form clusters. As the concentration of CTAB increases, the agglomeration gradually decreases and the morphology of the silica sample becomes more uniform. This proves that CTAB concentration is an important decision on the size, morphology and uniformity of SiO_2 after synthesis.

3.1.2. N_2 adsorption/desorption isotherms

The surface and textural properties of the adsorbents were measured using N_2 adsorption-/desorption isotherms (Fig. 4 and Table 1). Without the addition of CTAB, the SiO_2-0 sample has a small surface area and a low pore volume. The surface area, pore volume and average pore size of the SiO_2-1 sample are 98.2 m^2/g, 0.746 cm^3/g and 28.8 nm, respectively. At a higher content of CTAB, the surface area, pore volume and average pore size decrease slightly to 26.4 m^2/g, 0.116 cm^3/g and 18.1 nm, respectively, for SiO_2-5. When the CTAB content increases further, the surface area and pore volume increase. They are 496.4 m^2/g and 1.154 cm^3/g for SiO_2-10 and 544.5 m^2/g and 1.259 cm^3/g for SiO_2-15, respectively, but the average pore size of both samples

decreases to 9.3 and 9.4 nm, respectively. According to the IUPAC classification, the SiO_2-15 sample has hysteresis loop H3, which belongs to the type II isotherm, indicating the presence of slit-like holes in this material. In the 2-10 nm range, the pore size distribution shows two peaks, indicating a mesoporous material. The sample SiO_2-15, commonly referred to as SiO_2, was selected for the evaluation of adsorption performance.

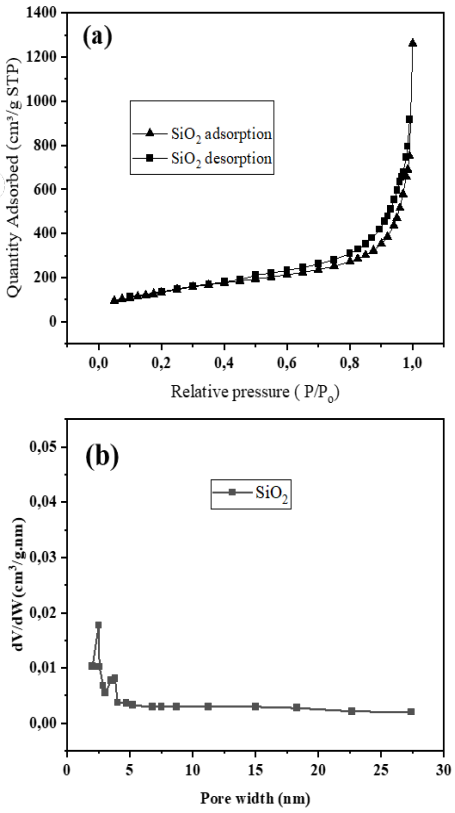

Fig. 4. (a) N_2 adsorption/desorption isotherms and (b) pore size distributions of SiO_2-15.

Table 1. Structure characteristic of the materials

Sample	S_{BET} (m^2/g)	Pore volume (cm^3/g)	Average pore size (nm)
SiO_2-0	15.2	0.161	55.4
SiO_2-1	98.2	0.746	28.8
SiO_2 -5	26.4	0.116	18.1
SiO_2 -10	496.4	1.154	9.3
SiO_2-15	544.5	1.289	9.4

3.1.3. TEM analysis

The morphology and size of the SiO_2 samples were analyzed using the TEM technique. It can be observed that the SiO_2-0 sample has particles with a size of 20 to 30 nm, with the particles lying close to each other. For SiO_2-15, the silica nanoparticles with a size of 10-20 nm tend to aggregate into porous clusters. However, the tiny pores with a size in the range of 2 to 5 nm are formed by the combustion of CTAB while the large pores with a size of 10 to 25 nm are formed by the structural distribution of the silica particles (Fig. 5). This also proves the role of the surfactant CTAB in creating porosity for the material when it is added to the gelation process [10].

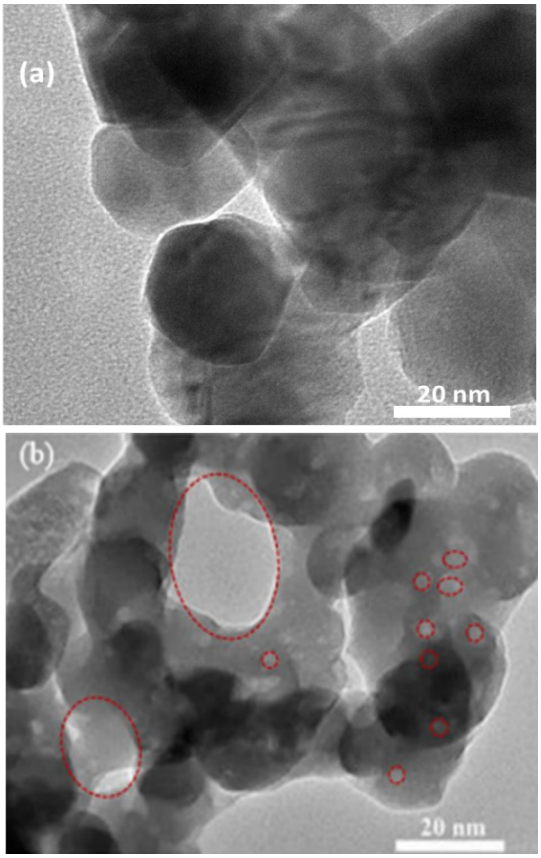

Fig. 5. The TEM images of SiO_2-0 and SiO_2-15.

3.1.4. XRD analysis

Fig. 6 shows the XRD patterns of SiO_2 samples. It can be seen that the peak intensity of the SiO-0 sample is higher than that of the other samples. However, all samples exhibit a diffraction peak with a large half spectrum at 24º, indicating that the silica prepared with and without CTAB is an amorphous material. In addition, no other peaks are observed, implying the purity of SiO_2. The result is also consistent with those of SiO_2 in previous reports [11].

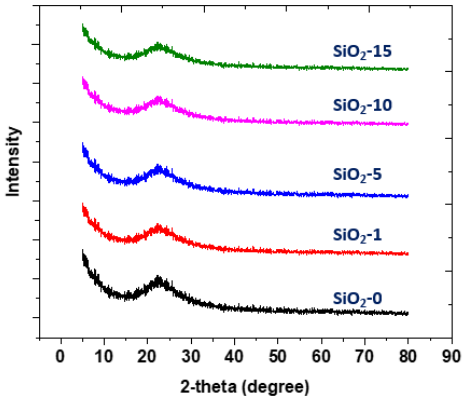

Fig. 6. XRD patterns of the SiO_2 samples.

3.2. Adsorption Performance SiO_2-15

3.2.1. Influence of exposure time

The experiment was carried out for 60 min under the specified reaction conditions (SiO_2 dosage of 0.5 g/L, pH=5.3, temperature of 30 °C). The removal of JGB from the solution with time is expressed in Fig. 7. The adsorption of JGB occurs rapidly in the initial 5 min and R_e reaches 93.8%. This can be explained by the availability of adsorption sites on the material surface. Thereafter, the adsorption process is relatively slow and shows the R_e value of 99.44% within 60 min.

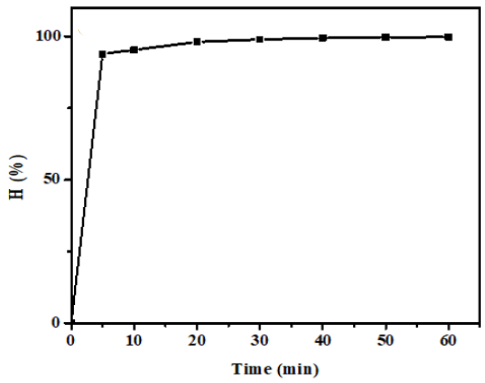

Fig. 7. Effect of contact time on JGB removal efficiency on SiO_2-15.

To determine the adsorption rate and rate-determining step, the kinetic of the dye adsorption process was investigated using first-and second-order kinetic models expressed as in following equations [12]:

First-order: $$ln(q_e - q_t) = lnq_e - k_1.t \quad (3)$$

Second-order: $$\frac{1}{q_t} = \frac{1}{k_2 q_e^2} + \frac{t}{q_e} \quad (4)$$

where q_e and q_t are the adsorption amount of JGB (mg/g) at time t and equilibrium, respectively, k_1 (min^{-1}) and k_2 ($g.mg^{-1}.min^{-1}$) is the rate constant.

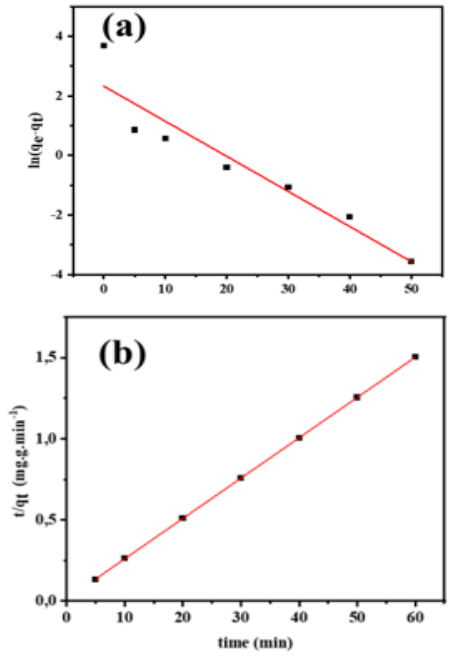

Fig. 8. (a) and (b) First-and second-order kinetic models for the adsorption of JGB on the SiO_2-15, respectively.

Fig. 8(a-b) present the plots of first and second-order kinetic model. The correlation coefficient (R^2) values of the first- and second-order models are 0.900 and 0.999, respectively. The k_1 and k_2 values are 0.118 min^{-1} and 0.054 $g.mg^{-1}.min^{-1}$, respectively. In addition, the q_e value of the second-order kinetic model is 40.21 (mg/g), which is close to the $q_{e,cal}$ (39.90 mg/g). These mean that the second-order kinetic model is more suitable to describe the adsorption of JGB on silica. The adsorption process takes place in two different stages. The first stage from 0 to 5 min corresponds to the instantaneous adsorption process or the adsorption occurring at the outer surface, in which an electron exchange take place between the adsorbent and the adsorbate. The second stage is the adsorption equilibrium, which occurs because the adsorption process begins to slow down and the material surface becomes saturated.

3.2.2. Influence of initial solution pH

In practical applications, all reaction parameters contribute to the adsorption process. In particular, the pH of the solution is one of the most important parameters for the adsorption process of JGB on SiO_2 since it not only affects the equilibrium level of the substances but also strongly influences the protonation of the surface groups and the degree of ionization of the adsorbents. The pH value is also an important factor in wastewater treatment. The pH of the solution was varied from 2 to 12 while the reaction conditions were fixed (SiO_2 dosage of 0.5 g/L, JGB concentration of 20 mg/L, temperature of 30 °C).

When the pH of the solution increases from 2 to 12, the adsorption increases and shows removal efficiencies of 69.42, 77.07, 99.91, 99.99, 99.97, and 99.99%, respectively (Table 2).

Table 2. Parameters for JGB adsorption influenced by pH.

Sample	k_2 g.mg^{-1}.min^{-1}	R^2	Removal efficiency (%)
pH=2	0.0355	0.999	69.42
pH=4	0.0318	0.999	77.07
pH=6	0.0250	1.000	99.91
pH=8	0.0249	1.000	99.99
pH=10	0.0250	1.000	99.74
pH=12	0.0248	0.999	99.99

It implied that base solution was favorable for the JGB removal process. At low pH, the higher H^+ concentration in the solution and they tend to protonate the adsorption sites, which leads to decreased removal efficiency. When pH is greater than 6, removal efficiencies at pH of 6, 8, 10 and 12 are similar, but pH of 6 is chosen as the optimal condition and for further research because basic environments will be costly for neutralization of wastewater in practical applications of dye treatment.

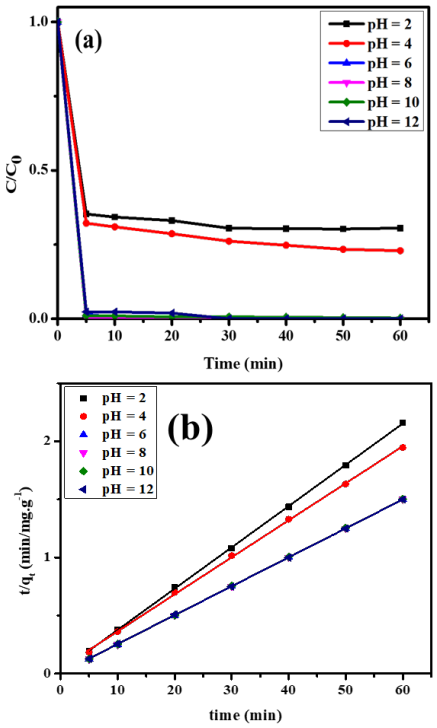

Fig. 9. (a) Effect of initial solution pH on the adsorption of JGB on SiO_2-15, (b) kinetic curves.

3.2.3. Influence of SiO_2-15 dosage

The influence of the SiO_2 dosage on the removal JGB is shown in Fig. 10. At a dose of 0.1 g/L, the removal efficiency and rate constant were 78.67% and 0.03 g.mg^{-1}.min^{-1}, respectively. These values increase to 99.83% and 0.025 g.mg^{-1}.min^{-1} at a dose of 0.5 g/L. This can be explained by the increase in surface area and the availability of biosorption sites. However, a further increase in the dose of SiO_2 (greater than 0.5 g/L) dose not lead to a further improvement in adsorption performance. Several factors may have contributed to this behavior, including aggregation, diffusion limitations, and hindered mass transfer. Therefore, the optimal dosage of 0.5 g/L was chosen.

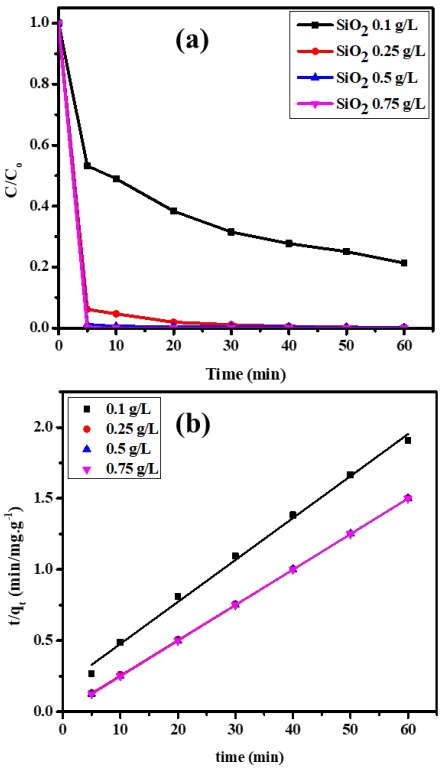

Fig. 10. (a) Removal efficiency and (b) second-order fitting curves with adsorbent dosage.

3.2.4. Influence of initial JGB concentration

The experiment was carried out for 60 min under the specified reaction conditions (SiO_2 dosage of 0.5 g/L, pH = 6, temperature of 30 °C), the result is presented in Fig. 11. The removal efficiency increases slightly when the concentration increases from 5 to 10 ppm and decreases slightly at concentration of 30 ppm. It is 99.05, 99.98, and 98.83% at concentrations of 5, 10, and 30 ppm, respectively. However, the $q_{e,cal}$ values are 9.91, 19.99 and 59.30 mg/g at concentrations of 5, 10, and 30 ppm, respectively. As the JGB concentration increases, the number of available adsorption sites may be limited. However, it can be observed that the higher the initial concentration, the greater the probability of collision

with adsorption sites on the surface of adsorbent. This is a great advantage for the adsorption capacity because the available adsorption sites can be saturated. Thus, when both removal efficiency and adsorption capacity are taken into account, the optimum JGB concentration is 30 ppm. Under optimal conditions, the adsorption occurs very quickly in the first 5 min then increases slightly and reaches equilibrium in 20 min. This is evidenced by the absorption spectrum of JGB with time in Fig. 11 (c).

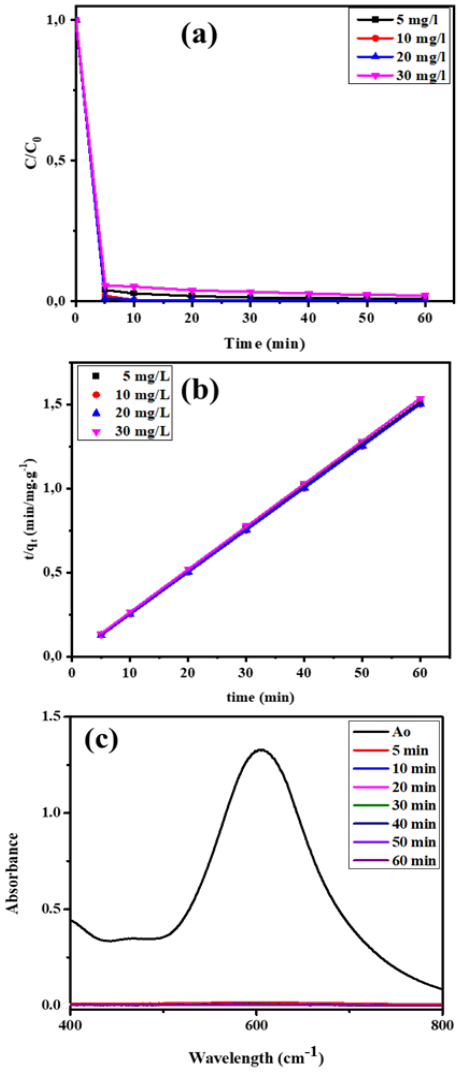

Fig. 11. (a) Removal efficiency, (b) second-order fitting curves with JGB concentration, and (c) UV-Vis spectrum of JGB under optimal conditions with time.

4. Conclusion

In summary, porous silica was successfully synthesized from rice husks with different contents of CTAB. The SiO_2 samples thus produced are amorphous and mesoporous material. Without the addition of CTAB, the surface area, pore volume and porosity are relatively low, which is significantly improved with CTAB. The formation of micelles and the combustion of CTAB can result in mesoporous structure of silica materials. The surface area, pore volume and average pore size are 544.5 m^2/g, 1.259 cm^3/g and 9.4 nm for SiO_2-15, respectively. The optimal conditions for the adsorption process are a solution a pH of 6, a SiO_2 dosage of 0.5 g/L and a JGB concentration of 30 ppm. The removal efficiency, adsorption capacity and rate constant are 98.83%, 59.30 mg/g and 0.025 $g.mg^{-1}.min^{-1}$, respectively. The adsorption is fast in the initial 5 min and then almost reaches equilibrium in 20 min, which is very favorable for large-scale applications.

Acknowledgements

The work was performed at the Vietnam Germany Catalysis Centre - RoHan Project funded by the German Academic Exchange Service (DAAD, No. 57315854) and the Federal Ministry for Economic Cooperation and Development (BMZ) inside the framework “SDG Bilateral Graduate school programme”.

References

[1] K. Qamar, G. Nchasi, H. T. Mirha, J. A. Siddiqui, K. Jahangir, S.K. Shaeen, Z. Islam, M.Y. Essar, Water sanitation problem in Pakistan: A review on disease prevalence, strategies for treatment and prevention, Annals of Medicine Surgery, vol. 2022, no. 82, Oct. 2012, pp. 104709. https://doi.org/10.1016/j.amsu.2022.104709

[2] N. A. Khan, H. J. An, D. K. Yoo, S. H. Jhung, Polyaniline-derived porous carbons: Remarkable adsorbent for removal of various hazardous organics from both aqueous and non-aqueous media, Journal of Hazardous Materials, vol. 360, Oct. 2018, pp. 163-171. https://doi.org/10.1016/j.jhazmat.2018.08.001

[3] W. Xiao, X. Jiang, X. Liu, W. Zhou, Z. N. Garba, I. Lawan, L. Wang, Z. Yuan, Adsorption of organic dyes from wastewater by metal-doped porous carbon materials, Journal of Cleaner Production, vol. 284, Feb. 2021, pp. 124773. https://doi.org/10.1016/j.jclepro.2020.124773

[4] P.N. Diagboya, B.I. Olu-Owolabi, K.O. Adebowale, Microscale scavenging of pentachlorophenol in water using amine and tripolyphosphate-grafted SBA-15 silica: Batch and modeling studies, Journal of Environmental Management, vol. 146, no. 100, Dec. 2014, pp. 42-49. https://doi.org/10.1016/j.jenvman.2014.04.038

[5] C.-H. Huang, K.-P. Chang, H.-D. Ou, Y.-C. Chiang, C.- F. Wang, Adsorption of cationic dyes onto mesoporous silica, Microporous and Mesoporous Materials, vol. 141, no. 1-3, May. 2011, pp. 102-109. https://doi.org/10.1016/j.micromeso.2010.11.002

[6] I. V. Melnyk, V. V. Tomina, N. V. Stolyarchuk, G. A. Seisenbaeva, V. G. Kessler, Organic dyes (acid red, fluorescein, methylene blue) and copper(II) adsorption on amino silica spherical particles with tailored surface hydrophobicity and porosity, Journal of Molecular Liquids, vol. 336, Aug. 2021, pp. 116301. https://doi.org/10.1016/j.molliq.2021.116301

[7] S. Ghosh, V. B. Vandana, Nano-structured mesoporous silica/silver composite: Synthesis, characterization and targeted application towards water purification, Materials Research Bulletin, vol. 88, Apr. 2017, pp. 291-300. https://doi.org/10.1016/j.materresbull.2016.12.044

[8] H. Thu, L. Dat, V. Anh Tuan, Synthesis of mesoporous SiO2 from rice husk for removal of organic dyes in aqueous solution, Vietnam Journal of Chemistry, vol. 57, Apr. 2019, pp. 175-181. https://doi.org/10.1002/vjch.201900012

[9] V.A.Tuan, V.V.Tu, Preparation of MgO for removal of dyes and heavy metal from aqueous solution: facially controlling the morphology, kinetic, isotherms and thermal dynamic investigations, Indian journal of Science and Technology, vol. 11, no. 41, Nov. 2018, pp. 1-5. https://doi.org/10.17485/ijst/2018/v11i41/131018

[10] N. V. Doan, V. T. Cuong, T. H. Nguyen, T. X. Do, A.-T. Vu, Preparation of novel CS/SiO2-EDTA nanocomposite from ash of rice straw pellets for enhanced removal efficiency of heavy metal ions in aqueous medium, Journal of Water Process Engineering, vol. 60, Apr. 2024, pp. 105175. https://doi.org/10.1016/j.jwpe.2024.105175

[11] S. Tabatabaei, A. Shukohfar, R. Aghababazadeh, A. Mirhabibi, Experimental study of the synthesis and characterisation of silica nanoparticles via the sol-gel method, Journal of Physics: Conference Series, vol. 26, no. 1, Feb. 2006, pp. 371. https://doi.org/10.1088/1742-6596/26/1/090

[12] A.-T. Vu, M.V. Nguyen, T.H. Nguyen, Fabrication of ethylenediaminetetraacetic modified porous silica composite from rice husk for enhancing the remove of Pb2+ from aqueous solution, Results in Materials, vol. 21, Mar. 2024, pp. 100525. https://doi.org/10.1016/j.rinma.2023.100525